



|                  |  |
|------------------|--|
| Title            | Medium effects on $\Xi(-)$ production in the nuclear ( $K^-$ , $K^+$ ) reaction  |
| Author(s)        | Harada, Toru; Hirabayashi, Yoshiharu   |
| Citation         | Physical Review C, 102(2), 024618<br><a href="https://doi.org/10.1103/PhysRevC.102.024618">https://doi.org/10.1103/PhysRevC.102.024618</a> |
| Issue Date       | 2020-08-17   |
| Doc URL          | <a href="http://hdl.handle.net/2115/79545">http://hdl.handle.net/2115/79545</a>  |
| Rights           | ©2020 American Physical Society  |
| Type             | article  |
| File Information | PhysRevC.102.024618.pdf  |



[Instructions for use](#)

## Medium effects on $\Xi^-$ production in the nuclear ( $K^-, K^+$ ) reaction

Toru Harada<sup>1,2,\*</sup> and Yoshiharu Hirabayashi<sup>3</sup>

<sup>1</sup>Research Center for Physics and Mathematics, Osaka Electro-Communication University, Neyagawa, Osaka 572-8530, Japan

<sup>2</sup>J-PARC Branch, KEK Theory Center, Institute of Particle and Nuclear Studies, High Energy Accelerator Research Organization (KEK), 203-1 Shirakata, Tokai, Ibaraki 319-1106, Japan

<sup>3</sup>Information Initiative Center, Hokkaido University, Sapporo 060-0811, Japan



(Received 17 February 2020; accepted 31 July 2020; published 17 August 2020)

We study theoretically medium effects on  $\Xi^-$  production in the ( $K^-, K^+$ ) reaction, using the optimal Fermi-averaging procedure, which describes the Fermi motion of a nucleon on the on-energy-shell  $K^-p \rightarrow K^+\Xi^-$  reaction condition in nuclei. The results show the strong energy and angular dependencies of the in-medium  $K^-p \rightarrow K^+\Xi^-$  cross section, which affect significantly the shape and the magnitude of the production spectrum for  $\Xi^-$ -hypernuclear states in the ( $K^-, K^+$ ) reaction on a nuclear target. The application to the  $\Xi^-$  quasifree production via the ( $K^-, K^+$ ) reaction on a  $^{12}\text{C}$  target is also discussed in a Fermi gas model.

DOI: [10.1103/PhysRevC.102.024618](https://doi.org/10.1103/PhysRevC.102.024618)

### I. INTRODUCTION

It is important to understand properties of  $\Xi$  hypernuclei whose states are regarded as the opening of the  $S = -2$  world in nuclear physics. This is a significant step to extend studies of multistrangeness systems and also strange neutron stars in astrophysics [1]. Recently, Nakazawa *et al.* [2] reported the first evidence of a bound state of the  $\Xi^-$ - $^{14}\text{N}$  system that was identified by the “KISO” event in the KEK-E373 experiment. This result supported that the  $\Xi$ -nucleus potential has a weak attraction of  $V_{\Xi} \simeq 14$  MeV in the Wood-Saxon potential, as suggested by previous analyses [3–5]. However, there still remains an uncertainty about the nature of the  $S = -2$  dynamics caused by the  $\Xi N$  interaction and also  $\Xi N - \Lambda\Lambda$  coupling in nuclei due to the limit to the available data. More experimental information is needed for the understanding of  $\Xi^-$  hypernuclei.

A pioneer study of  $\Xi$  hypernuclei by Dover and Gal [6] indicated that a  $\Xi$ -nucleus potential has a well depth of  $V_{\Xi} = 24 \pm 4$  MeV based on the analysis of old emulsion data. Khaustov *et al.* [5] discussed a missing mass spectrum near the  $\Xi$  threshold in the  $^{12}\text{C}(K^-, K^+)$  reaction at 1.8 GeV/ $c$  in the BNL-E885 experiment. Their analysis showed  $V_{\Xi} \simeq 14$  MeV for the  $\Xi$ -nucleus potential, whereas the resolution was not sufficient to resolve  $\Xi^-$ -hypernuclear states. Recently, Nagae *et al.* [7] have performed an accurate observation of the  $\Xi^-$ -production spectrum in the  $^{12}\text{C}(K^-, K^+)$  reaction at 1.8 GeV/ $c$  in the J-PARC E05 experiment, and this analysis is now ongoing.

On the other hand, the authors of Refs. [8–10] discussed the  $\Sigma^-$ -nucleus potential in the quasifree (QF) spectra of the ( $\pi^-, K^+$ ) reactions on the nuclear targets, using the optimal Fermi-averaging procedure [11]. This procedure describes the Fermi motion of a nucleon on the on-energy-shell  $\pi^-p \rightarrow K^+\Sigma^-$  reaction condition in nuclei, and it generates the

energy dependence of the in-medium  $\pi^-p \rightarrow K^+\Sigma^-$  reaction amplitude. This energy dependence due to the Fermi motion leads to a successful explanation of the ( $\pi^-, K^+$ ) spectra in the distorted-wave impulse approximation analyses of  $^{28}\text{Si}$  [8],  $^{209}\text{Bi}$  [9], and  $^6\text{Li}$  [10] targets; it is possible to extract properties of the  $\Sigma$ -nucleus potential appropriately from the experimental data in nuclear ( $\pi^-, K^+$ ) reactions. Therefore, it is worthwhile studying the medium effects on  $\Xi^-$  production in the nuclear ( $K^-, K^+$ ) reactions, employing the optimal Fermi-averaging procedure.

Maekawa *et al.* [12] investigated the  $\Xi^-$  QF spectra in the ( $K^-, K^+$ ) reaction on  $^{12}\text{C}$  in similar calculations considering the local momentum for the nucleon and  $\Xi$ . Hashimoto *et al.* [13] also discussed the  $\Xi^-$  QF spectra in the ( $K^-, K^+$ ) reactions on  $^{12}\text{C}$  in the semiclassical distorted wave (SCDW) method. Recently, Kohno [14] has reexamined the  $\Xi^-$  QF spectra in the ( $K^-, K^+$ ) reactions on  $^9\text{Be}$  and  $^{12}\text{C}$  targets in the SCDW method, using the  $\Xi$ -nucleus potential derived from the next-to-leading order in chiral effective field theory. However, it seems that the calculated  $\Xi^-$  QF spectra are insufficient to reproduce the data quantitatively.

In this paper, we study theoretically medium effects on  $\Xi^-$  production in the nuclear ( $K^-, K^+$ ) reaction. We evaluate the in-medium cross sections of the  $K^-p \rightarrow K^+\Xi^-$  reaction, using the optimal Fermi-averaging procedure [11], and we discuss the energy and angular dependence of the  $\Xi^-$ -production spectrum in the ( $K^-, K^+$ ) reaction on a nuclear target. We also apply this procedure to the  $\Xi^-$  QF production spectrum in the ( $K^-, K^+$ ) reaction on a  $^{12}\text{C}$  target at  $p_{K^-} = 1.8$  GeV/ $c$  in a Fermi gas model.

### II. CALCULATIONS

#### A. Distorted-wave impulse approximation

Let us consider a calculation procedure of the hypernuclear production for the nuclear ( $K^-, K^+$ ) reaction in the laboratory frame. The inclusive double-differential cross sections within

\*harada@osakac.ac.jp

the distorted-wave impulse approximation (DWIA) [15,16] are given by (in units  $\hbar = c = 1$ )

$$\frac{d^2\sigma}{dE_{K^+}d\Omega_{K^+}} = \beta \frac{1}{[J_A]} \sum_{m_A} \sum_{B,m_B} |\langle \Psi_B | \hat{F} | \Psi_A \rangle|^2 \times \delta(\omega - E_B + E_A), \quad (1)$$

where  $[J] = 2J + 1$ , and  $\Psi_B$  and  $\Psi_A$  ( $E_B$  and  $E_A$ ) are wave functions (energies) of hypernuclear final states and an initial state of the target nucleus, respectively. The laboratory energy transfer and the momentum transfer are

$$\omega = E_{K^-} - E_{K^+}, \quad \mathbf{q} = \mathbf{p}_{K^-} - \mathbf{p}_{K^+}, \quad (2)$$

where  $E_{K^-}$  and  $\mathbf{p}_{K^-}$  ( $E_{K^+}$  and  $\mathbf{p}_{K^+}$ ) denote an energy and a momentum of the incoming  $K^-$  (the outgoing  $K^+$ ), respectively. The energy transfer may also be expressed as

$$\omega = E_B - E_A = m_{\Xi^-} - m_N - B_{\Xi^-} - \varepsilon_N + T_{\text{recoil}}, \quad (3)$$

where  $B_{\Xi^-}$  is a  $\Xi^-$  binding energy,  $\varepsilon_N$  is a single-particle energy of a nucleon-hole state, and  $T_{\text{recoil}}$  is a recoil energy to the final state. The kinematical factor  $\beta$  [3] arising from a translation from a two-body meson-nucleon laboratory system to a meson-nucleus laboratory system [6] is given by

$$\beta = \left( 1 + \frac{E_{K^+}^{(0)} p_{K^+}^{(0)} - p_{K^-}^{(0)} \cos \theta_{\text{lab}}}{E_B^{(0)} p_{K^+}^{(0)}} \right) \frac{p_{K^+} E_{K^+}}{p_{K^+} E_{K^+}}, \quad (4)$$

where  $p_{K^-}^{(0)}$  and  $p_{K^+}^{(0)}$  ( $E_{K^+}^{(0)}$  and  $E_B^{(0)}$ ) are laboratory momenta of  $K^-$  and  $K^+$  (laboratory energies of  $K^+$  and  $\Xi^-$ ) in the two-body  $K^-p \rightarrow K^+\Xi^-$  reaction, respectively. Here we considered only the non-spin-flip reaction because the spin-flip contribution seems to be not so large in the ( $K^-$ ,  $K^+$ ) reaction. Thus an external operator  $\hat{F}$  for the associated production  $K^-p \rightarrow K^+\Xi^-$  reactions is given by

$$\hat{F} = \int d\mathbf{r} \chi_{p_{K^+}}^{(-)*}(\mathbf{r}) \chi_{p_{K^-}}^{(+)}(\mathbf{r}) \times \sum_{j=1}^A \bar{f}_{K^-p \rightarrow K^+\Xi^-} \delta(\mathbf{r} - \mathbf{r}_j) \hat{O}_j, \quad (5)$$

with zero-range interaction for the  $K^-p \rightarrow K^+\Xi^-$  transitions.  $\chi_{K^+}^{(-)*}$  and  $\chi_{K^-}^{(+)}$  are distorted waves of incoming  $K^-$  and outgoing  $K^+$ , respectively.  $\hat{O}_j$  is a baryon operator changing the  $j$ th nucleon into a  $\Xi^-$  hyperon in the nucleus,  $\mathbf{r}$  is the relative coordinate between the mesons and the center-of-mass (c.m.) of the nucleus, and  $\bar{f}_{K^-p \rightarrow K^+\Xi^-}$  is the in-medium  $K^-p \rightarrow K^+\Xi^-$  amplitude on the laboratory frame.

In the DWIA, a Fermi-averaged amplitude is often used for  $\bar{f}_{K^-p \rightarrow K^+\Xi^-}$  so as to take into account a Fermi motion in the nuclear medium [16]. However, it should be noted that the energy dependence of  $\bar{f}_{K^-p \rightarrow K^+\Xi^-}$  may play an important role in describing the QF spectrum within a wide energy range ( $\sim$  a few hundred MeV) as well as the angular dependence. The authors of Refs. [8–10] emphasized the importance of the energy dependence of the Fermi-averaged amplitude of  $\bar{f}_{\pi^-p \rightarrow K^+\Sigma^-}$  in the nuclear ( $\pi^-$ ,  $K^+$ ) reactions to extract properties of the  $\Sigma$ -nucleus potential from the experimental data, using the optimal Fermi-averaging procedure [11]. Therefore,

we are interested in the energy dependence and the angular dependence of  $\bar{f}_{K^-p \rightarrow K^+\Xi^-}$ , which is generated by the optimal Fermi-averaging procedure in the nuclear ( $K^-$ ,  $K^+$ ) reaction.

## B. Optimal Fermi averaging

According to Ref. [11], we consider the optimal Fermi averaging for the  $K^-p \rightarrow K^+\Xi^-$  reaction in a nucleus. To see clearly the medium effects of the  $K^-p \rightarrow K^+\Xi^-$  processes in the nuclear ( $K^-$ ,  $K^+$ ) reaction in the framework of the DWIA, we introduce an ‘‘optimal’’ cross section for the  $K^-p \rightarrow K^+\Xi^-$  processes in the nucleus, which can be given as

$$\left( \frac{d\sigma}{d\Omega} \right)_{\theta_{\text{lab}}}^{\text{opt}} \equiv \beta |\bar{f}_{K^-p \rightarrow K^+\Xi^-}|^2 = \frac{p_{K^+} E_{K^+}}{(2\pi)^2 v_{K^-}} |t_{\bar{K}N, K\Xi}^{\text{opt}}(p_{K^-}; \omega, \mathbf{q})|^2, \quad (6)$$

where  $v_{K^-} = p_{K^-}/E_{K^-}$ . The optimal Fermi-averaged  $\bar{K}N \rightarrow K\Xi$   $t$  matrix,  $t_{\bar{K}N, K\Xi}^{\text{opt}}(p_{K^-}; \omega, \mathbf{q})$ , is defined by

$$t_{\bar{K}N, K\Xi}^{\text{opt}}(p_{K^-}; \omega, \mathbf{q}) = \frac{\int_0^\pi \sin \theta_N d\theta_N \int_0^\infty dp_N p_N^2 \rho(p_N) t_{\bar{K}N, K\Xi}(E_2; \mathbf{p}_{\bar{K}}, \mathbf{p}_N)}{\int_0^\pi \sin \theta_N d\theta_N \int_0^\infty dp_N p_N^2 \rho(p_N)} \Bigg|_{p_N = p_N^*}, \quad (7)$$

where  $E_N$  and  $\mathbf{p}_N$  are an energy and a momentum of a proton in the target nucleus, respectively;  $\cos \theta_N = \hat{\mathbf{p}}_{\bar{K}} \cdot \hat{\mathbf{p}}_N$ ;  $E_2 = E_{K^-} + E_N$  is the total energy of the  $K^-N$  system; and  $\rho(p_N)$  is a Fermi-momentum distribution of the proton in the target nucleus. The momentum  $\mathbf{p}_N^*$  in Eq. (7) is a solution which satisfies the on-energy-shell equation for a struck proton in the nuclear systems,

$$\sqrt{(\mathbf{p}_N^* + \mathbf{q})^2 + m_{\Xi}^2} - \sqrt{(\mathbf{p}_N^*)^2 + m_N^2} = \omega, \quad (8)$$

where  $m_{\Xi}$  and  $m_N$  are masses of  $\Xi^-$  and the proton, respectively. This procedure keeps the on-energy-shell  $K^-p \rightarrow K^+\Xi^-$  processes in the nucleus [17]; thus it guarantees to take ‘‘optimal’’ values for  $\bar{f}_{K^-p \rightarrow K^+\Xi^-}$  within a factorized form, e.g., see Eq. (12). Note that binding effects for the nucleon and  $\Xi$  in the nucleus are considered automatically when we input experimental values for the binding energies of the nuclear and hypernuclear states in Eq. (3). Here we neglected the energy dependence of a phase for the  $K^-p \rightarrow K^+\Xi^-$   $t$  matrix and replaced  $t_{\bar{K}N, K\Xi}(E_2; \mathbf{p}_{\bar{K}}, \mathbf{p}_N)$  in the laboratory frame by its absolute value  $|t_{\bar{K}N, K\Xi}(E_2; \mathbf{p}_{\bar{K}}, \mathbf{p}_N)|$ , which is obtained from the corresponding one in the c.m. frame;  $t_{\bar{K}N, K\Xi}(E_2; \mathbf{p}_{\bar{K}}, \mathbf{p}_N) = \eta t_{\text{c.m.}}(E_{\text{c.m.}})$ , where  $\eta$  is the Möller factor. Such an assumption has been confirmed to be appropriate in the case of the  $\pi^+n \rightarrow K^+\Lambda$  process in the nuclear ( $\pi^+$ ,  $K^+$ ) reactions [11].

## C. $K^-p \rightarrow K^+\Xi^-$ reaction

In the optimal Fermi-averaging procedure, we need to prepare the elementary  $K^-p \rightarrow K^+\Xi^-$   $t$  matrices (amplitudes), which fully reproduce the experimental data of differential cross sections in free space. Recently, several authors [18,19] have investigated the  $K^-p \rightarrow K^+\Xi^-$  reaction amplitudes, of

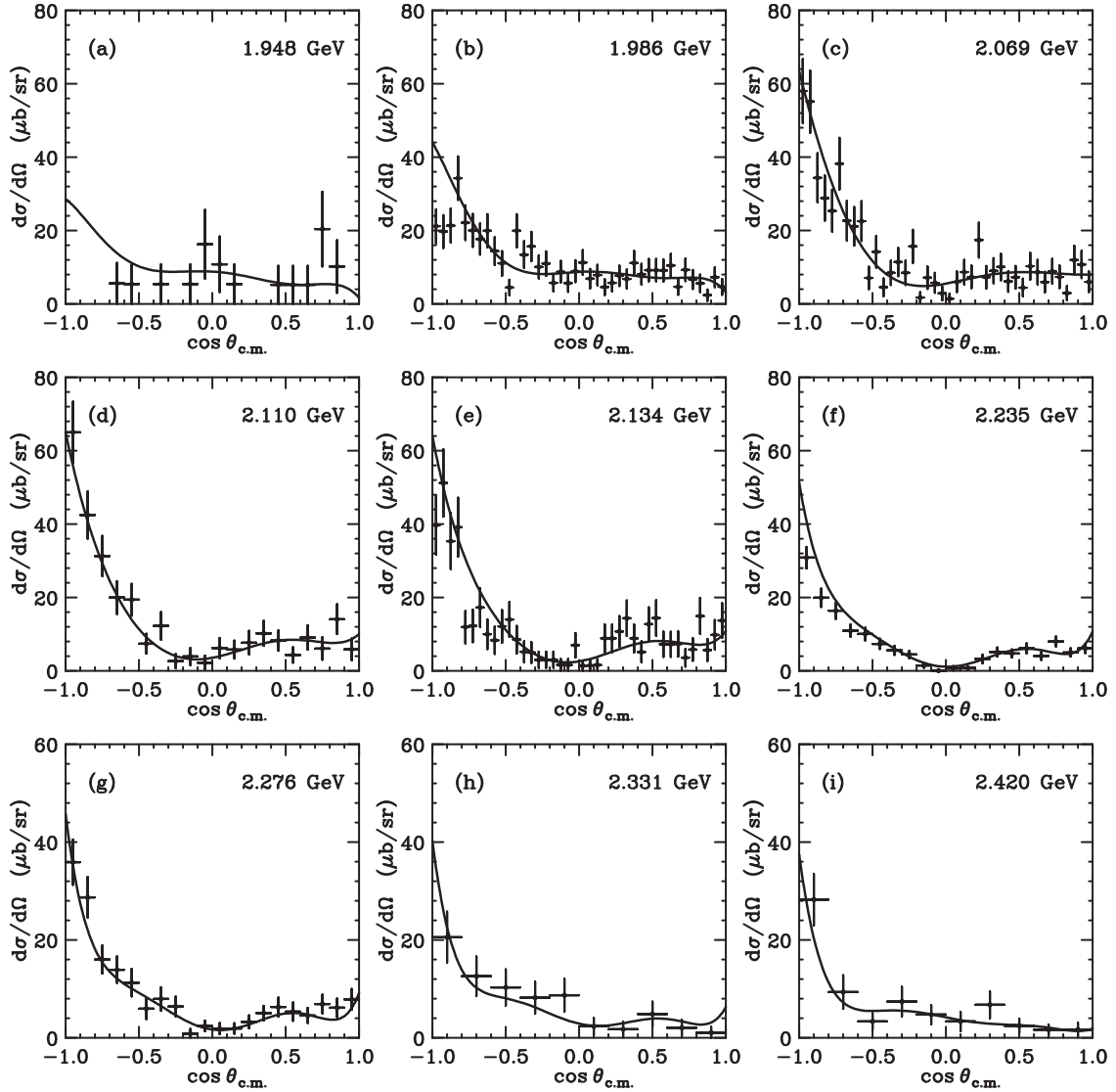


FIG. 1. Angular distributions of the differential cross section for the  $K^-p \rightarrow K^+\Xi^-$  reaction in the c.m. frame at  $E_{c.m.} = 1.948, 1.966, 2.069, 2.110, 2.134, 2.235, 2.276, 2.331,$  and  $2.420$  GeV. Solid curves denote the calculated values to make a fit to the experimental data. The data are taken from Refs. [21–25], following the compilation in Ref. [18].

which the nature is caused by  $Y^*$  resonances as intermediate states via the  $K^-p \rightarrow K^+\Xi^-$  processes, by the help of theoretical models due to poor quality in the available data [18–20]. However, we use the angular distributions of the  $K^-p \rightarrow K^+\Xi^-$  reaction for the sake of simplicity. They are parametrized according to

$$\begin{aligned} \left(\frac{d\sigma}{d\Omega}\right)_{c.m.}^{\text{elem}} &= \frac{\omega_f \omega_i p_f}{(2\pi)^2 p_i} |t_{c.m.}(E_{c.m.})|^2 \\ &= \lambda^2 \sum_{\ell=0}^{\ell_{\max}} A_{\ell}(E_{c.m.}) P_{\ell}(\cos \theta_{c.m.}), \end{aligned} \quad (9)$$

where  $t_{c.m.}(E_{c.m.})$  denotes the  $K^-p \rightarrow K^+\Xi^-$   $t$  matrix in the c.m. frame;  $p_f$  ( $p_i$ ) and  $\omega_f$  ( $\omega_i$ ) are a momentum and a reduced energy for  $K^+\Xi^-$  ( $K^-p$ ) in the c.m. frame, respectively;  $\lambda$  is the de Broglie wavelength of  $K^-p$ ; and  $P_{\ell}(x)$  are Legendre polynomials. Coefficient parameters  $A_{\ell}(E_{c.m.})$  are expressed

by a power series of  $E_{c.m.}$ , so as to make a fit to their energy dependence.

Figure 1 displays the angular distributions of  $(d\sigma/d\Omega)_{c.m.}^{\text{elem}}$ , together with the data at  $E_{c.m.} = 1.948, 1.966, 2.069, 2.110, 2.134, 2.235, 2.276, 2.331,$  and  $2.420$  GeV [21–25]. Here  $\ell_{\max} = 6$  is used. Figure 2 also displays the total (integrated) cross sections [20], which are written as

$$\begin{aligned} \sigma_{\text{tot}}(E_{c.m.}) &= \int d\Omega \left(\frac{d\sigma}{d\Omega}\right)_{c.m.}^{\text{elem}} \\ &= 4\pi \lambda^2 A_0(E_{c.m.}), \end{aligned} \quad (10)$$

as a function of  $E_{c.m.}$ . The parameters  $A_{\ell}(E_{c.m.})$  were determined for fits to 242 data points for the angular distributions of  $d\sigma/d\Omega$  in Fig. 1, together with nine data points (open circles in Fig. 2) for the total cross sections of  $\sigma_{\text{tot}}$  that were simultaneously measured with the data of  $d\sigma/d\Omega$ . Thus the renormalized  $\chi^2$  values account for  $\chi^2/N = 1.48$ , with

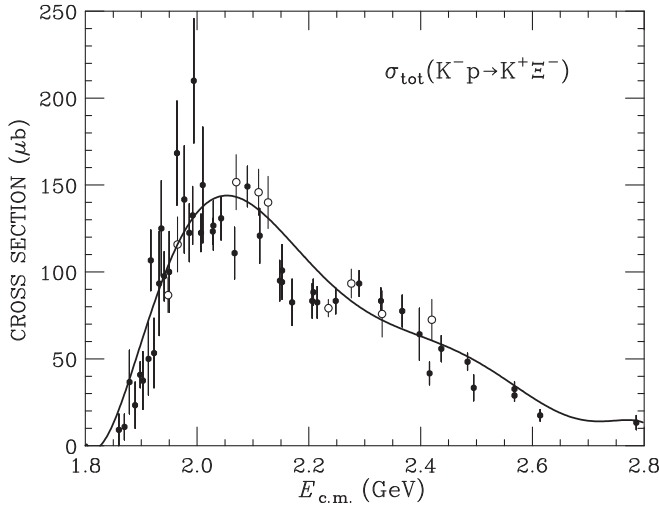


FIG. 2. Total cross section  $\sigma_{\text{tot}}$  for the  $K^- p \rightarrow K^+ \Xi^-$  reaction as a function of the energy  $E_{\text{c.m.}}$ . The data are taken from the compilation of Flaminio *et al.* [20]. Open and solid circles denote the data for  $\sigma_{\text{tot}}$  with and without the measurements of  $d\sigma/d\Omega$  shown in Fig. 1, respectively.

$N = 242$  for  $d\sigma/d\Omega$ , and  $\chi^2/N = 2.35$ , with  $N = 56$  (open and solid circles) for  $\sigma_{\text{tot}}$ .

Figure 3 shows the laboratory differential cross sections  $(d\sigma/d\Omega)^{\text{elem}}$  for the  $K^- p \rightarrow K^+ \Xi^-$  reaction at  $\theta_{\text{lab}} = 0^\circ - 16^\circ$ , as a function of the incident  $K^-$  momentum of  $p_{K^-}$ . We find that the values of  $(d\sigma/d\Omega)^{\text{elem}}$  rather depend on  $p_{K^-}$ . The peak of  $(d\sigma/d\Omega)^{\text{elem}}$  at  $\theta_{\text{lab}} = 0^\circ$  is located at  $p_{K^-} \approx 1.9$  GeV/c, and its position is shifted downward as  $\theta_{\text{lab}}$  increases. The peak of  $(d\sigma/d\Omega)^{\text{elem}}$  at  $\theta_{\text{lab}} = 16^\circ$  stands at  $p_{K^-} \approx 1.5$  GeV/c. Thus, the energy and angular dependencies of  $(d\sigma/d\Omega)^{\text{elem}}$  may affect the shape and the magnitude of the  $\Xi^-$ -production spectrum in the nuclear ( $K^-, K^+$ ) reaction at each  $\theta_{\text{lab}}$ .

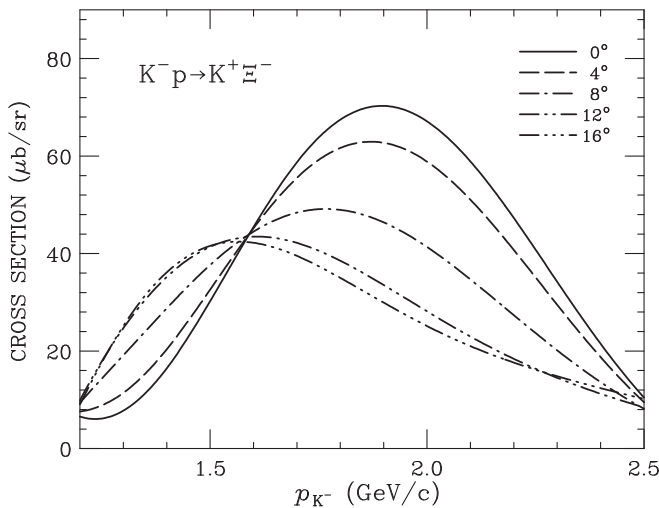


FIG. 3. Incident  $K^-$  momentum dependence of the laboratory differential cross sections for the  $K^- p \rightarrow K^+ \Xi^-$  reaction,  $(d\sigma/d\Omega)^{\text{elem}}$ , at  $\theta_{\text{lab}} = 0^\circ, 4^\circ, 8^\circ, 12^\circ$ , and  $16^\circ$ .

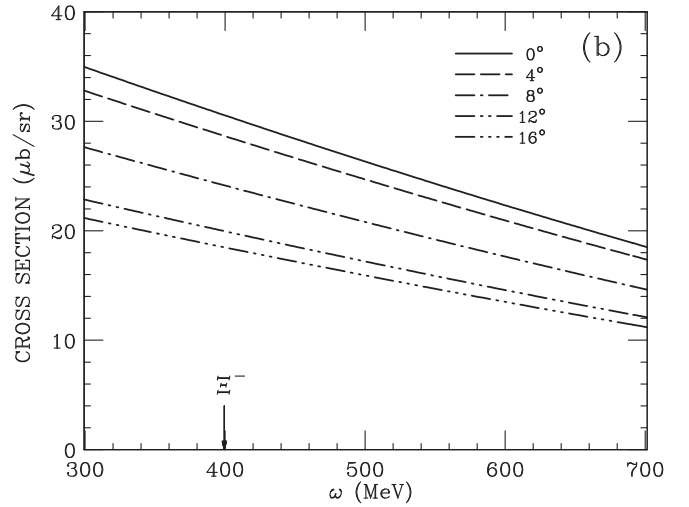
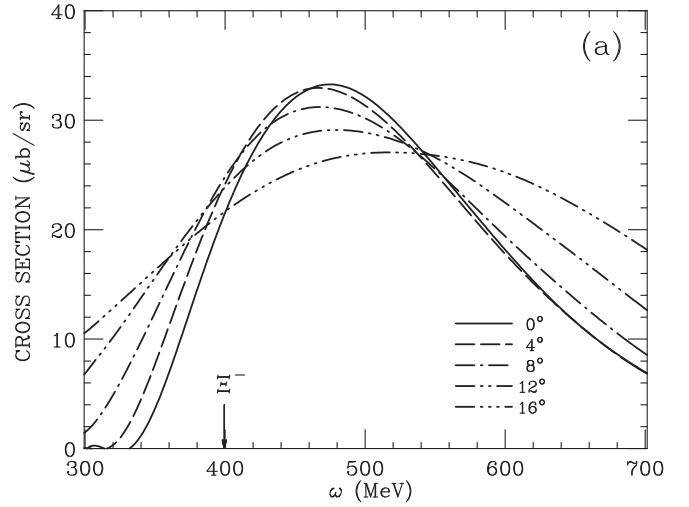


FIG. 4. Energy dependence of (a) the optimal Fermi-averaged cross section  $(d\sigma/d\Omega)^{\text{opt}}$  and (b) the ordinary Fermi-averaged cross section  $\beta(d\sigma/d\Omega)^{\text{av}}$  with the kinematical factor  $\beta$  of Eq. (4) for the  $K^- p \rightarrow K^+ \Xi^-$  reaction on the  $^{12}\text{C}$  target at  $p_{K^-} = 1.8$  GeV/c and  $\theta_{\text{lab}} = 0^\circ, 4^\circ, 8^\circ, 12^\circ$ , and  $16^\circ$ , as a function of the energy transfer  $\omega$ . The arrows show the  $\Xi^-$  emitted threshold.

### III. RESULTS AND DISCUSSION

#### A. Optimal Fermi-averaged cross section

To see the medium effects on the  $K^- p \rightarrow K^+ \Xi^-$  reaction in nuclei, we evaluate the optimal Fermi-averaged cross section of  $(d\sigma/d\Omega)^{\text{opt}}$  in the laboratory frame, referring to the values of  $(d\sigma/d\Omega)^{\text{elem}}$  of Eq. (9) in the optimal Fermi-averaging procedure. Figure 4(a) shows the calculated results of  $(d\sigma/d\Omega)^{\text{opt}}$  in the  $K^- p \rightarrow K^+ \Xi^-$  reaction at  $p_{K^-} = 1.8$  GeV/c and  $\theta_{\text{lab}} = 0^\circ - 16^\circ$  in kinematics for a  $^{12}\text{C}$  target, as a function of the energy transfer  $\omega$ . We find the strong energy dependence of  $(d\sigma/d\Omega)^{\text{opt}}$  for  $\omega$ , together with the angular dependence of them for  $\theta_{\text{lab}}$ . Note that the cross sections can be estimated in not only the  $\Xi^-$  continuum region but also the  $\Xi^-$  bound region due to the Fermi motion in the nuclear medium. The peak of  $(d\sigma/d\Omega)^{\text{opt}}$  is located at  $\omega \simeq 480$  MeV, which corresponds to  $E_{\Xi^-} \simeq 80$  MeV with



respect to the  $\Xi^-$  emitted threshold when  $\theta_{\text{lab}} = 0^\circ - 8^\circ$ , whereas the peak position moves upward as  $\theta_{\text{lab}}$  increases; when  $\theta_{\text{lab}} = 16^\circ$ , thus its position is located at  $\omega \simeq 520$  MeV ( $E_{\Xi^-} \simeq 120$  MeV). The behavior of  $(d\sigma/d\Omega)^{\text{opt}}$  can play a significant role in describing the shape and the magnitude of the  $\Xi^-$  spectrum in the nuclear ( $K^-, K^+$ ) reaction. It was found that the energy dependence and the angular dependence of  $(d\sigma/d\Omega)^{\text{opt}}$  are significant to describe the behavior of the  $\Lambda$ -production spectra in the nuclear ( $\pi^+, K^+$ ) reactions [11] and also the  $\Sigma^-$ -production ones in the nuclear ( $\pi^-, K^+$ ) reactions [8–10]. Therefore, the optimal Fermi-averaging procedure is expected to work well for describing the medium effects on the  $K^-p \rightarrow K^+\Xi^-$  reaction in nuclei.

In the standard DWIA in hypernuclear production theories [16,26,27], we often find the ‘‘ordinary’’ Fermi averaging in which the Fermi-averaged differential cross section for the  $K^-p \rightarrow K^+\Xi^-$  reaction may be given as

$$\left(\frac{d\sigma}{d\Omega}\right)_{\theta_{\text{lab}}}^{\text{av}} = \int d\mathbf{p}_N \rho(p_N) \left(\frac{d\sigma}{d\Omega}\right)^{\text{elem}}. \quad (11)$$

In Fig. 4(b), we show the calculated cross sections of  $\beta(d\sigma/d\Omega)^{\text{av}}$ , including the kinematical factor  $\beta$  of Eq. (4) at  $p_{K^-} = 1.8$  GeV/c for  $^{12}\text{C}$ , in comparison with those of  $(d\sigma/d\Omega)^{\text{opt}}$ . We confirm that the values of  $\beta(d\sigma/d\Omega)^{\text{av}}$  decrease monotonously due to the energy dependence of  $\beta$  [3], as  $\omega$  increases. Here we used, e.g., the values of  $(d\sigma/d\Omega)^{\text{av}} = 51.9$   $\mu\text{b/sr}$  at  $\theta_{\text{lab}} = 4^\circ$  and  $43.1$   $\mu\text{b/sr}$  at  $\theta_{\text{lab}} = 8^\circ$ . It is shown clearly that the values of  $\beta(d\sigma/d\Omega)^{\text{av}}$  are quite different from those of  $(d\sigma/d\Omega)^{\text{opt}}$  because the values of  $(d\sigma/d\Omega)^{\text{av}}$  depend on  $p_{K^-}$  and  $\theta_{\text{lab}}$ , not  $\omega$ .

On the other hand, it is known that the impulse approximation for nuclear reaction theories is improved to reduce the influence of the off-shell  $t$  matrix caused by the Fermi motion for a nucleon in the nuclear target by choosing an optimal momentum  $\mathbf{p}_N^{\text{opt}}$  for the nucleon [17,28]. This is called the optimal momentum approximation [17] in which the use of the on-shell  $t$  matrix may be valid because the leading-order correction due to Fermi motion is minimized. Several authors [29,30] have studied the effects of the Fermi motion in DWIA calculations for  $\Lambda$  hypernuclear production and have proposed to use the optimal momentum  $\mathbf{p}_N^{\text{opt}}$  for the nucleon in the target nucleus. This momentum may be given as  $\mathbf{p}_N^{\text{opt}} = (\eta - \frac{1}{2})\mathbf{q}$  in the laboratory frame where  $\eta$  is a factor determined at a frozen point for Fermi motion [28] instead of the Fermi averaging. However, their approach seems to be still insufficient to explain the influence of the energy dependence and the angular dependence of  $(d\sigma/d\Omega)^{\text{elem}}$  in a nuclear medium such as the  $K^-p \rightarrow K^+\Xi^-$  reaction, in a quantitative comparison with the experimental data of the hypernuclear production [29]. Consequently, we recognize that the optimal Fermi-averaging procedure is a straightforward way of dealing with the Fermi-averaged amplitude for the elementary reaction in the optimal momentum approximation.

### B. Application to $\Xi^-$ QF production on $^{12}\text{C}$ in a Fermi gas model

To see the medium effects in the nuclear ( $K^-, K^+$ ) reaction, we demonstrate the  $\Xi^-$  QF spectrum in the ( $K^-, K^+$ ) reaction

on a nuclear target, using the calculated results of  $(d\sigma/d\Omega)^{\text{opt}}$  in Eq. (6). We adopt a nonrelativistic Fermi gas model [31], in which each nucleon moves freely in the field of a uniform nuclear potential well  $V$ , for simplicity. The QF spectrum in  $\Lambda$  hypernuclear production via the ( $K^-, \pi^-$ ) reaction was first evaluated by Dalitz and Gal [32]. The  $\Lambda$  QF spectrum for the associated ( $\pi^+, K^+$ ) reaction in terms of the high-momentum transfer was also discussed by Dover *et al.* [27]. Following Refs. [27,31], the double-differential cross section in the nuclear ( $K^-, K^+$ ) reaction in Eq. (1) may be rewritten as

$$\frac{d^2\sigma}{dE_{K^+}d\Omega_{K^+}} = \left(\frac{d\sigma}{d\Omega}\right)^{\text{opt}} R(\omega, \mathbf{q}). \quad (12)$$

The response function  $R(\omega, \mathbf{q})$  is defined as

$$R(\omega, \mathbf{q}) = Z_{\text{eff}} \frac{3}{4\pi k_F^3} \int d\mathbf{p}_N \theta(k_F - |\mathbf{p}_N|) \times \delta\left(\bar{\omega} - \frac{(\mathbf{p}_N + \mathbf{q})^2}{2m_\Xi} + \frac{\mathbf{p}_N^2}{2m_N}\right), \quad (13)$$

where  $k_F$  is the Fermi momentum,  $\mathbf{p}_N$  is the momentum for the nucleon, and  $\bar{\omega} = \omega - (m_\Xi - m_N) - (V_N - V_\Xi)$ . In the eikonal approximation, the effective number of protons  $Z_{\text{eff}}$  may be approximated by

$$Z_{\text{eff}} = \int d\mathbf{r} \rho_A(r) |\chi_{p_{K^+}}^{(-)}(\mathbf{r})|^2 |\chi_{p_{K^-}}^{(+)}(\mathbf{r})|^2 \approx \int d\mathbf{b} T_p(\mathbf{b}) \exp[-\bar{\sigma}T(\mathbf{b})], \quad (14)$$

where the nuclear thickness function is defined as

$$T(\mathbf{b}) \equiv \int_{-\infty}^{\infty} \rho(\mathbf{r}) dz, \quad \int T(\mathbf{b}) d\mathbf{b} = A. \quad (15)$$

Here  $\mathbf{b}$  is an impact-parameter coordinate in the plane perpendicular to the direction of the momentum transfer  $\mathbf{q}$ ;  $T_p(\mathbf{b})$  is a thickness function for the proton, thus  $\int T_p(\mathbf{b}) d\mathbf{b} = Z$ . The averaged total cross section for the  $K^-N$  and  $K^+N$  elastic scatterings is given as  $\bar{\sigma} = \frac{1}{2}(\sigma_{K^-N} + \sigma_{K^+N})$ . Note that  $Z_{\text{eff}}$  reduces to the proton number  $Z$  for the limit of no distortion ( $\bar{\sigma} \rightarrow 0$ ).

Considering  $q > k_F$  because  $q \simeq 390 - 800$  MeV/c ( $\theta_{\text{lab}} = 0^\circ - 16^\circ$ ) in the nuclear ( $K^-, K^+$ ) reaction, the response function in Eq. (13) is easily obtained as

$$R(\omega, \mathbf{q}) = Z_{\text{eff}} \frac{3}{4\pi} \left(\frac{m_\Xi}{k_F^2}\right) \frac{\pi}{\sqrt{Q^2 - 4\alpha^2(v - Q^2/2)}} \times \left\{ 1 - \frac{1}{4\alpha^4} (Q - \sqrt{Q^2 - 4\alpha^2(v - Q^2/2)})^2 \right\} \quad (16)$$

for  $Q > 2\alpha^2$ , where the dimensionless valuables of  $Q = q/k_F$ ,  $\alpha^2 = (m_\Xi - m_N)/2m_N$ , and  $v = m_\Xi \bar{\omega}/k_F^2$ ; we confirm that for small  $Q$ ,  $R(\omega, \mathbf{q})$  is proportional to  $1/Q\{1 - (v/Q - Q/2)^2\}$ , a well-known parabolic function [31], as well as for  $\alpha^2 \rightarrow 0$  ( $m_\Xi/m_N \rightarrow 1$ ). The peak of this response occurs

at  $v = Q^2/2 + \alpha^2$  or

$$\omega_{\text{peak}} = m_{\Xi} - m_N + (V_N - V_{\Xi}) + \frac{m_{\Xi} - m_N}{m_{\Xi}} \frac{k_F^2}{2m_N} + \frac{q^2}{2m_{\Xi}}, \quad (17)$$

and its width  $2\Delta = 2k_F q/m_{\Xi}$ , whereas this position may be moderated in the  $\Xi^-$  spectrum of Eq. (12) due to the energy dependence of  $(d\sigma/d\Omega)^{\text{opt}}$  or  $\beta(d\sigma/d\Omega)^{\text{av}}$ .

Now let us estimate the  $\Xi^-$  QF spectrum in the  $(K^-, K^+)$  reaction on the  $^{12}\text{C}$  target at  $p_{K^-} = 1.8 \text{ GeV}/c$ . For distortion, we use  $\bar{\sigma} = 24.2 \text{ mb}$  as the parameter, where  $\sigma_{K^-} = 28.9 \text{ mb}$  for  $K^-N$  scattering and  $\sigma_{K^+} = 19.4 \text{ mb}$  for  $K^+N$  scattering [8,9]. When we use the modified harmonic oscillator density for  $^{12}\text{C}$ , which is written as

$$\rho(r) = \rho_0 \{1 + a(r/d)^2\} \exp\{-(r/d)^2\}, \quad (18)$$

with  $a = 2.234$  and  $d = 1.516 \text{ fm}$  [33], we find  $Z_{\text{eff}} = 2.09$ , evaluating Eq. (14) numerically by the eikonal-wave integral [6,27]. For  $p_{K^-} = 1.8 \text{ GeV}/c$  and  $\theta_{\text{lab}} = 4^\circ$ , thus, we estimate  $\bar{\omega}_{\text{peak}} \simeq 542 \text{ MeV}$  and  $2\Delta \simeq 222 \text{ MeV}$  consistently, using  $q \simeq 542 \text{ MeV}/c$  at  $\omega = 537 \text{ MeV}$  for  $^{12}\text{C}$ . Here we took masses of  $m_N = 938.27 \text{ MeV}$  for the proton and  $m_{\Xi} = 1321.71 \text{ MeV}$  for the  $\Xi^-$  hyperon, the attractive well depths of  $V_N = 50 \text{ MeV}$  and  $V_{\Xi} = 14 \text{ MeV}$ , and the Fermi momentum of  $k_F = 270 \text{ MeV}/c$  in the nucleus. We also consider the recoil correction in the spectrum, replacing  $q$  by  $q_{\text{eff}} = (M_C/M_A)q$ , where  $M_A$  and  $M_C$  denote the masses of the  $^{12}\text{C}$  target and the  $^{11}\text{B}$  core nuclei, respectively [34].

In Fig. 5, we show the calculated  $\Xi^-$  QF spectra of Eq. (12) in the  $^{12}\text{C}(K^-, K^+)$  reaction at  $p_{K^-} = 1.8 \text{ GeV}/c$ ,  $\theta_{\text{lab}} = 4^\circ$  and  $8^\circ$ . The calculated spectrum at  $\theta_{\text{lab}} = 4^\circ$  has a QF peak at  $\omega \simeq 480 \text{ MeV}$ , which corresponds to about 80 MeV above the  $\Xi^-$  emitted threshold, and a width of  $2\Delta \simeq 150 \text{ MeV}$ , which is extremely narrower than that of  $2\Delta \simeq 200 \text{ MeV}$  for the spectrum with  $\beta(d\sigma/d\Omega)^{\text{av}}$ . For  $\theta_{\text{lab}} = 8^\circ$ , the QF peak position slightly shifts upward ( $\omega \simeq 500 \text{ MeV}$ ) and its width becomes  $2\Delta \simeq 200 \text{ MeV}$ . We find that the  $\omega$  dependence of  $(d\sigma/d\Omega)^{\text{opt}}$  acts on the shape and the magnitude of the QF spectrum remarkably, and it makes its width narrower, in comparison with that of  $\beta(d\sigma/d\Omega)^{\text{av}}$  as well as that in the case of  $\beta(d\sigma/d\Omega)^{\text{av}} = \text{const.}$ , which is proportional to  $R(\omega, q)$ . The magnitude of the spectrum seems to be rather as large as the magnitudes with  $\beta(d\sigma/d\Omega)^{\text{av}}$  in the forward angles ( $\theta_{\text{lab}} \leq 4^\circ$ ), whereas we find a considerable difference among the shapes of these spectra near the  $\Xi^-$  emitted threshold. Consequently, we realize that the optimal Fermi-averaged amplitudes of  $\bar{f}_{K^-p \rightarrow K^+\Xi^-}$  in Eq. (5) allow one to moderate directly the shape and the magnitude of the spectrum including the  $\Xi^-$  QF region with a wide energy range. Thus it is required to extract information concerning the  $\Xi^-$ -nucleus potential carefully from the data of the experimental spectrum.

Moreover, it should be mentioned that there still remain some uncertainties about the values of  $(d\sigma/d\Omega)^{\text{elem}}$  due to the limit of the available data of the  $K^-p \rightarrow K^+\Xi^-$  reaction. Thus if we use the different parameters of  $A_\ell(E_{\text{c.m.}})$  in Eq. (10) that simulate the values of  $\sigma_{\text{tot}}$  predicted in Ref. [19], we find that the shape of the calculated values of  $(d\sigma/d\Omega)^{\text{opt}}$  is modified and the magnitude is reduced by about 20% in the

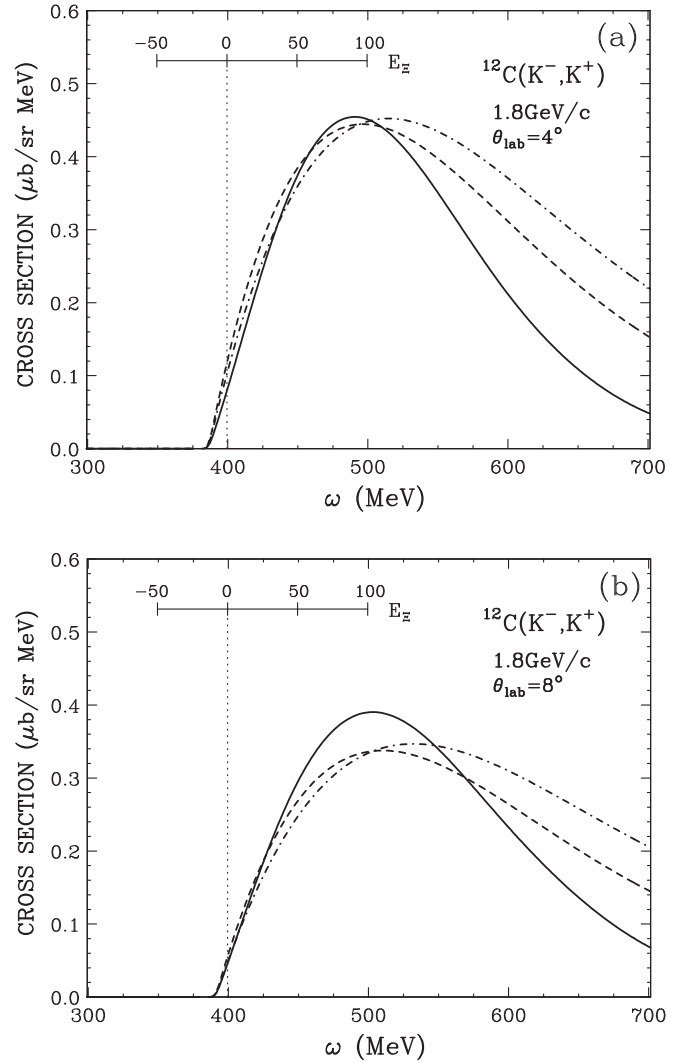


FIG. 5. The  $\Xi^-$  QF production spectra in the Fermi gas model in the  $^{12}\text{C}(K^-, K^+)$  reaction at  $p_{K^-} = 1.8 \text{ GeV}/c$ , (a)  $\theta_{\text{lab}} = 4^\circ$  and (b)  $8^\circ$ , as a function of the energy transfer  $\omega$ . Solid, dashed, and dot-dashed curves denote the calculated results of the spectra with  $(d\sigma/d\Omega)^{\text{opt}}$ ,  $\beta(d\sigma/d\Omega)^{\text{av}}$ , and the constant value of  $\beta(d\sigma/d\Omega)^{\text{av}} = 31.1$  (25.9)  $\mu\text{b}/\text{sr}$  at  $\theta_{\text{lab}} = 4^\circ$  ( $8^\circ$ ), respectively. The spectra are folded with a detector resolution of 5 MeV full width at half maximum.

region of  $\omega \simeq 400\text{--}500 \text{ MeV}$  above the  $\Xi^-$  emitted threshold. This implies the ability to judge the validity of  $(d\sigma/d\Omega)^{\text{elem}}$  if our approach satisfies completely a description of the  $\Xi^-$  spectrum in the  $(K^-, K^+)$  reaction. An attempt at such studies may need a more quantitative observation of the differential cross sections in the elementary  $p(K^-, K^+)\Xi^-$  reaction and the nuclear  $(K^-, K^+)$  reaction experimentally.

### C. Applicability of the optimal Fermi averaging

We study the applicability of the optimal Fermi-averaging procedure to the inclusive  $(K^-, K^+)$  reactions by high momentum  $K^-$  beams because the contribution of two-step processes may grow in the inclusive reactions on heavier

nuclear targets [35,36]. We recognize that the optimal Fermi-averaged  $t$  matrix provides the benefit of the optimal momentum approximation [17], as already mentioned in Sec. III A. Considering the general relation between the exact scattering operator  $\tau$  and an approximate one,  $t_a$ , which is written as

$$\begin{aligned} \tau = & t_a + t_a G_a h G_a t_a \\ & + t_a G_a h (G_a + G_a t_a G_a) h G_a t_a + \dots \end{aligned} \quad (19)$$

in terms of the expansion series with  $h \equiv G_a^{-1} - G^{-1}$ , where  $G$  and  $G_a$  are exact and approximate Green's functions, respectively, we confirm that the contribution from the first-order correction term of  $t_a G_a h G_a t_a$  vanishes in the optimal momentum approximation [17]. As far as the  $\Xi^-$  production is concerned in the inclusive ( $K^-, K^+$ ) reactions, this correction may correspond to the two-step processes of  $K^-N \rightarrow K^-N$  followed by  $K^-p \rightarrow K^+\Xi^-$  or  $K^-p \rightarrow K^+\Xi^-$  followed by  $K^+N \rightarrow K^+N$ , involving rescattering effects in nuclear medium. It implies that the optimal Fermi-averaged  $t$  matrix  $t_{\bar{K}N, K\Xi}^{\text{opt}}$  inevitably includes medium effects due to these two-step processes. Therefore, we expect that the optimal Fermi-averaging procedure works well within the impulse approximation for the  $\Xi^-$  production on light nuclei and also on heavier nuclei in which strong absorption and distortion effects must be taken into account.

On the other hand, if we consider strangeness productions with various hyperons ( $Y = \Xi, \Xi^*, \Lambda, \Sigma, \dots$ ) in the inclusive ( $K^-, K^+$ ) reactions, it is necessary to deal with additional optimal Fermi-averaged  $t$  matrices for the corresponding reactions, e.g.  $\bar{K}N \rightarrow \bar{K}N, KN \rightarrow KN, \bar{K}N \rightarrow YM$  ( $Y^*M$ ) followed by  $MN \rightarrow YK$  ( $Y^*K^*$ ), because the contributions of the two-step processes with intermediate mesons ( $M = \pi, K, \bar{K}, \phi, a_0$ , and  $f_0$ ) and hyperon resonances are very important [36]. We believe that our procedure can be extended to the

additional two-step processes for the strangeness productions in the inclusive ( $K^-, K^+$ ) reactions.

#### IV. SUMMARY AND CONCLUSION

We have studied theoretically the medium effects on the  $\Xi^-$  production via the  $K^-p \rightarrow K^+\Xi^-$  process in the nuclear ( $K^-, K^+$ ) reaction, using the optimal Fermi-averaging procedure. The calculated optimal Fermi-averaged amplitudes of  $\bar{f}_{K^-p \rightarrow K^+\Xi^-}$  for our DWIA calculations provide the strong energy and angular dependencies, leading to the fact that the shape and the magnitude of the  $\Xi^-$ -production spectrum is influenced in the ( $K^-, K^+$ ) reaction on a nuclear target. We have also demonstrated the  $\Xi^-$  QF spectrum in the  $^{12}\text{C}(K^-, K^+)$  reaction at  $p_{K^-} = 1.8 \text{ GeV}/c$  within the Fermi gas model.

In conclusion, we show the strong energy and angular dependencies of the in-medium  $K^-p \rightarrow K^+\Xi^-$  production cross section, which is important to describe the shape and the magnitude of the  $\Xi^-$ -production spectrum in the ( $K^-, K^+$ ) reaction on the nuclear target. This result may be a basis for study extracting the properties of the  $\Xi$ -nucleus potential from the experimental data. The detailed investigations are required for the analysis of the  $^{12}\text{C}(K^-, K^+)$  reaction at  $1.8 \text{ GeV}/c$  at the J-PARC E05 experiment [7] and also for the extension to the two-step processes in the inclusive ( $K^-, K^+$ ) reactions. These investigations are subjects for future research.

#### ACKNOWLEDGMENTS

The authors thank Prof. T. Fukuda, Prof. T. Nagae, and Prof. Y. Akaishi for many valuable discussions. This work was supported by Grants-in-Aid for Scientific Research (KAKENHI) from the Japan Society for the Promotion of Science (Grant No. JP20K03954).

- 
- [1] D. Chatterjee and I. Vidana, *Eur. Phys. J. A* **52**, 29 (2016).
  - [2] K. Nakazawa *et al.*, *Prog. Theor. Exp. Phys.* **2015**, 033D02 (2015).
  - [3] S. Tadokoro, H. Kobayashi, and Y. Akaishi, *Phys. Rev. C* **51**, 2656 (1995).
  - [4] T. Fukuda *et al.* (E224 Collaboration), *Phys. Rev. C* **58**, 1306 (1998).
  - [5] P. Khaustov *et al.* (The AGS E885 Collaboration), *Phys. Rev. C* **61**, 054603 (2000).
  - [6] C. B. Dover and A. Gal, *Ann. Phys.* **146**, 309 (1983).
  - [7] T. Nagae *et al.*, in *Proceedings of the 13th International Conference on Hypernuclear and Strange Particle Physics: HYP2018*, edited by L. Tang and R. Schumacher, AIP Conf. Proc. No. 2130 (AIP, New York, 2019), p. 020015.
  - [8] T. Harada and Y. Hirabayashi, *Nucl. Phys. A* **759**, 143 (2005).
  - [9] T. Harada and Y. Hirabayashi, *Nucl. Phys. A* **767**, 206 (2006).
  - [10] T. Harada, R. Honda, and Y. Hirabayashi, *Phys. Rev. C* **97**, 024601 (2018).
  - [11] T. Harada and Y. Hirabayashi, *Nucl. Phys. A* **744**, 323 (2004).
  - [12] H. Maekawa, K. Tsubakihara, and A. Ohnishi, *Eur. Phys. J. A* **33**, 269 (2007).
  - [13] S. Hashimoto, M. Kohno, K. Ogata, and M. Kawai, *Prog. Theor. Phys.* **119**, 1005 (2008).
  - [14] M. Kohno, *Phys. Rev. C* **100**, 024313 (2019).
  - [15] J. Hüfner, S. Y. Lee, and H. A. Weidenmüller, *Nucl. Phys. A* **234**, 429 (1974).
  - [16] E. H. Auerbach *et al.*, *Ann. Phys. (NY)* **148**, 381 (1983).
  - [17] S. A. Gurvitz, *Phys. Rev. C* **33**, 422 (1986).
  - [18] D. A. Sharov, V. L. Korotkikh, and D. E. Lansky, *Eur. Phys. J. A* **47**, 109 (2011).
  - [19] B. C. Jackson, Y. Oh, H. Haberzettl, and K. Nakayama, *Phys. Rev. C* **91**, 065208 (2015).
  - [20] V. Flaminio, I. F. Graf, J. D. Hansen, W. G. Moorhead, and D. R. O. Morrison, CERN-HERA Report 79-02 (CERN, Geneva, 1979).
  - [21] W. P. Trower, J. P. Ficenec, R. I. Hulsiger, J. Lathrop, J. N. Snyder, and W. P. Swanson, *Phys. Rev.* **170**, 1207 (1968).
  - [22] G. Burgun *et al.*, *Nucl. Phys. B* **8**, 447 (1968).
  - [23] P. M. Dauber, J. P. Berge, J. R. Hubbard, D. W. Merrill, and R. A. Muller, *Phys. Rev.* **179**, 1262 (1969).
  - [24] T. G. Trippe and P. E. Schlein, *Phys. Rev.* **158**, 1334 (1967).
  - [25] G. W. London, R. R. Rau, N. P. Samios, S. S. Yamamoto, M. Goldberg, S. Lichtman, M. Prime, and J. Leitner, *Phys. Rev.* **143**, 1034 (1966).



- [26] H. Bandō, T. Motoba, and J. Žofka, *Int. J. Mod. Phys. A* **5**, 4021 (1990).
- [27] C. B. Dover, L. Ludeking, and G. E. Walker, *Phys. Rev. C* **22**, 2073 (1980).
- [28] X. Q. Zhu, N. Mobed, and S. S. M. Wong, *Nucl. Phys. A* **466**, 623 (1987).
- [29] J. Žofka, M. Sotona, and V. N. Fetisov, *Nucl. Phys. A* **431**, 603 (1984).
- [30] M. Sotona, J. Žofka, V. N. Fetisov, and H. Bandō, *Czech. J. Phys. B* **39**, 1273 (1989).
- [31] T. de Forest, Jr., and J. D. Walecka, *Adv. Phys.* **15**, 1 (1966).
- [32] R. H. Dalitz and A. Gal, *Phys. Lett. B* **64**, 154 (1976).
- [33] E. Friedman, A. Gal, and C. J. Batty, *Nucl. Phys. A* **579**, 518 (1994).
- [34] T. Harada and Y. Hirabayashi, *Phys. Rev. C* **100**, 024605 (2019).
- [35] T. Iijima *et al.*, *Nucl. Phys. A* **546**, 588 (1992).
- [36] Y. Nara, A. Ohnishi, T. Harada, and A. Engel, *Nucl. Phys. A* **614**, 433 (1997).